

MSEC2016-8766

POLISHING CHARACTERISTICS OF TRANSPARENT POLYCRYSTALLINE YAG CERAMICS USING MAGNETIC FIELD-ASSISTED FINISHING

Daniel Ross, Yanming Wang, Hadyan Ramadhan, Hitomi Yamaguchi
Department of Mechanical and Aerospace Engineering, University of Florida
Gainesville, FL, USA

ABSTRACT

Transparent polycrystalline yttrium aluminum garnet (YAG) ceramics have garnered an increased level of interest for high-power laser applications due to their ability to be manufactured in large sizes, and doped in relatively substantial concentrations when compared to traditional single-crystalline gain media. However, surface characteristics have a direct effect on the lasing ability of these materials, and a lack of a fundamental understanding of the polishing mechanisms of these ceramics remains a challenge for their utilization. The aim of this paper is to study the polishing characteristics of YAG ceramics using magnetic field-assisted finishing (MAF). An experimental setup was developed, through the refinement of the MAF process, for YAG ceramic workpieces. Using this equipment with diamond abrasives, the YAG ceramic surfaces were polished to sub-nanometer scale. Polishing trials with fine diamond abrasive and colloidal silica were then performed on this sub-nanometer surface and the material removal mechanisms were analyzed.

Polishing with 0-0.1 μm diameter diamond abrasive caused increasing roughness with polishing time due to the continuous cycle of relatively substantial chipping followed by minor smoothing. Polishing with colloidal silica caused valleys to widen with increased polishing time and the grain structure of the ceramic influenced the material removal.

INTRODUCTION

Solid state lasers have traditionally used single-crystalline gain media. The first such example was a ruby based laser created by Maiman in 1960 [1,2]. Continuous-wave laser oscillation utilizing single crystal Nd:YAG was successfully accomplished not long after in 1964 [3]. Translucent YAG ceramics were developed as gain media in the 1980's, however they performed poorly due to low-optical-grade properties [4-6]. It wasn't until the mid-1990's when Ikesue *et al.* developed transparent Nd:YAG ceramics of high enough optical quality to produce successful laser oscillation [7]. Since this time it has been shown that laser oscillations can be obtained with YAG ceramics which are comparable or even superior to those of single-crystalline YAG [8,9]. Polycrystalline gain media can be scaled to much larger sizes, are relatively economical, and can undergo heavy doping [10-13]. As such, polycrystalline host

materials have garnered an increased level of interest for high-power applications.

These advanced ceramics, however, have structural challenges that must be overcome. Conventional polycrystalline ceramics have a variety of light scattering sources which can result in lower laser power output and slope efficiencies. Refractive index modulation can occur at the grain boundaries and any inclusions or pores can cause index changes. Birefringence can be a concern, as well as scattering at the surface caused by roughness [14,15]. The internal scattering sources have been diminished substantially with modern fabrication techniques, however surface roughness can still have great effects on lasing ability. In addition to the scattering that can occur due to surface roughness, it has been shown that laser threshold is greatly affected by surface conditions [16]. Surface characteristics are also very important when bonding the ceramics to make a larger composite or when applying coatings. Defects in the bonding zone or under the coating can cause internal scattering centers in the interior of these composites. Since the surface finish of polycrystalline YAG ceramics is heavily involved in lasing performance it is necessary to understand the polishing characteristics of this material.

Poly- and single-crystalline materials have been polished by a variety of techniques. Diamond is an often utilized abrasive due to its relative hardness to the ceramics. Colloidal silica is also used for the polishing of ceramics due to its ability to chemically react with ceramic materials and reduce sub-surface damage [17]. To better control the polishing of polycrystalline YAG ceramic, it is important to clarify the material removal mechanisms that these abrasives have on this material.

Magnetic field-assisted finishing (MAF) has arisen as a promising technology for overcoming problems associated with more traditional polishing techniques. Through control of magnetic fields, magnetic particles and abrasives can be navigated against and across surfaces with precision. Magnetic field-assisted finishing techniques have been shown to be successful in the fine finishing of optical components [18], and ultra-fine finishes were achieved using MAF on thin quartz wafers [19]. The MAF process lends itself to precision polishing as well as localized material removal and is thus a potentially favorable technique for laser gain media.

This paper discusses the refinement of the MAF process for the polishing of YAG ceramics. Moreover, this paper discusses the effects and material removal mechanisms of diamond and colloidal silica abrasives on polycrystalline YAG ceramics using MAF.

PROCESSING PRINCIPLE

Figure 1 shows a schematic of the MAF processing principle used for wafer finishing. A permanent magnet is attached to a rotating table at a specific offset from the axis of rotation, referred to as eccentricity. This acts as the magnetic field generator and will be referred to as the table magnet. The workpiece is secured to a holder above the rotating table and iron particles are placed on the workpiece. An additional permanent magnet (referred to as the tool magnet) is put on the iron particles. The iron particles align with the magnetic field lines generated between the table magnet and tool magnet creating a free form brush. Abrasives are then introduced into the finishing zone between the iron brush and the workpiece surface. The magnetic force F acting on the tool magnet and iron particles, pressing the abrasives against the surface, is described by Eq. (1)

$$F = V\chi H \cdot \text{grad}H \quad (1)$$

where V is the volume of the magnetic particle, χ is the susceptibility, and H and $\text{grad}H$ are the intensity and gradient of the magnetic field, respectively. Through modifying the volume of the magnetic particles as well as the magnetic properties, size, and arrangement of the magnets utilized the polishing force can be controlled.

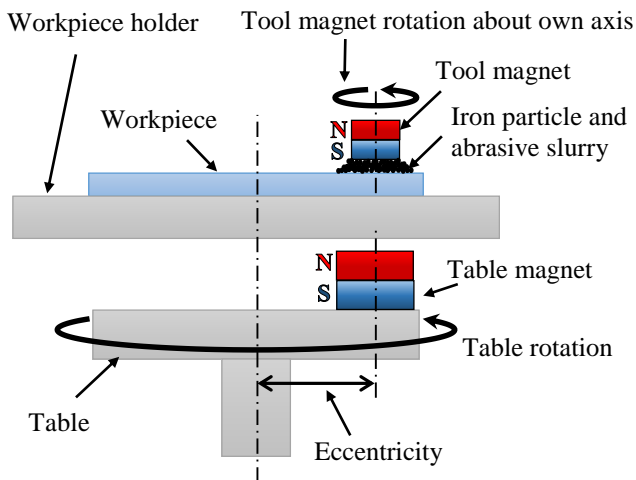
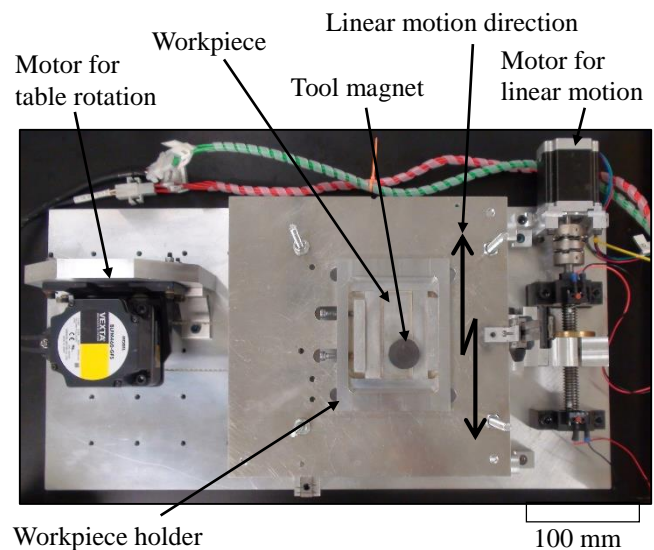


FIGURE 1 - MAF PROCESSING PRINCIPLE SCHEMATIC

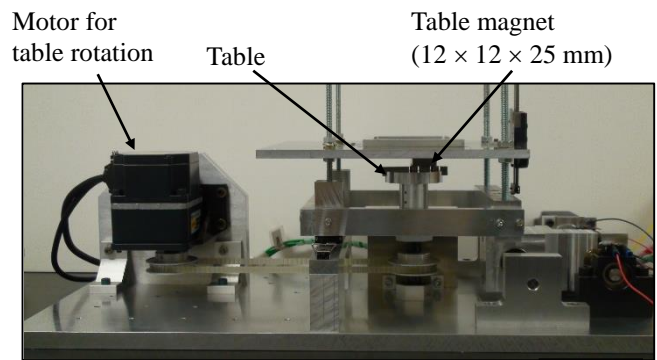
As the table magnet rotates about a central axis, the tool magnet and iron particles are pulled across the surface of the workpiece providing the motion required for finishing. In addition to the tool magnet rotating about the table magnets rotational axis, the tool magnet rotates about its own central axis. This phenomenon is referred to as self-spinning and is caused by a tangential velocity gradient across the tool magnet as it follows the table magnet. The self-spinning of the tool magnet creates

intersecting cut marks and encourages the introduction of fresh abrasive cutting edges.

The experimental setup, displayed in Fig. 2, was developed to realize this processing principle (with some refinements) for the polishing of polycrystalline YAG ceramic slabs. For example, due to the hardness and relative thickness (7.4 mm) of the YAG ceramic, a large polishing force is required compared to the force required for 60 μm thick quartz polishing [19]. Nd-Fe-B rare earth tool and table magnets were thus selected. The workpiece is held in place by a non-ferrous holder and the permanent table magnet is placed on a ferrous bar fixed to the rotating table. The distance between the bottom of the holder and table magnet is adjustable and the holder table can move linearly, allowing for the polishing of the entire rectangular area of the surface.



(a) Top view



(b) Front View

FIGURE 2 – EXPERIMENTAL SETUP

As Fig. 3 shows, the iron particles initially line up along the lines of magnetic force between the tool magnet and workpiece surface. However, during rotation the iron particles gradually climb to the uppermost surface of the tool magnet. As the table magnet rotates, the tool magnet with iron particles is dragged

across the workpiece surface. The frictional force between the workpiece surface and loose iron particles naturally wants to drive the iron particles out of the interface between the tool magnet and workpiece surface. The iron particles in the interface push the iron particles near them, and the iron particles as a whole flow along the magnetic field lines to the top surface of the tool magnet. If nothing impedes this flow of iron particles, a majority will eventually leave the interface and the tool magnet will directly interact with the workpiece surface, damaging the workpiece. To prevent this from occurring, the tool magnet was fitted with a rubber magnet “cap” which has a diameter larger than the tool magnet. The cap is held securely to the uppermost surface of the tool magnet due to the strong magnetic force. This cap prevents the iron particles from being pushed to the top surface of the tool magnet by the iron particles in the interface. The iron particles cannot flow from the interface and the iron brush is maintained, preventing any contact between tool magnet and workpiece.

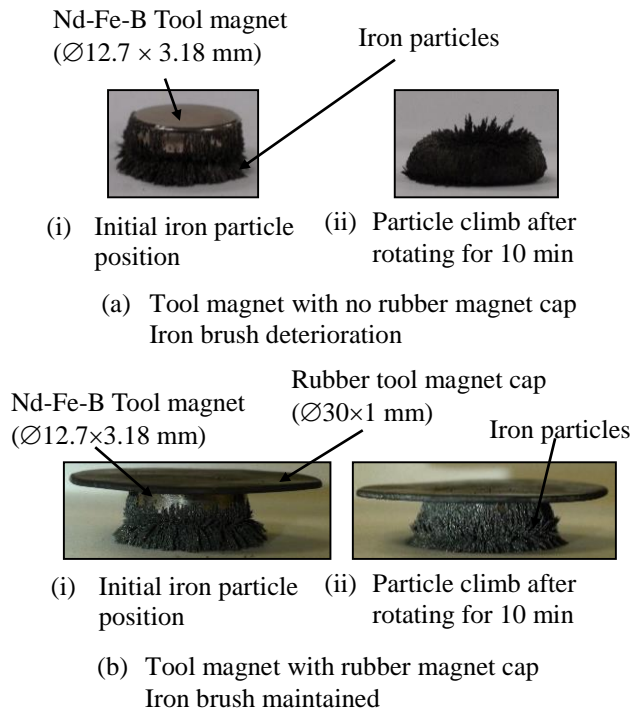
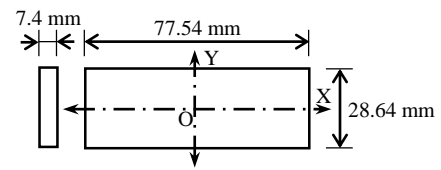


FIGURE 3 – TOOL MAGNET COMPONENTS AND IRON PARTICLE CLIMB

POLISHING CHARACTERISTICS

In this study, polishing experiments of polycrystalline YAG ceramic slabs focused on abrasive type, iron particle size, and polishing time. The first set of experiments carried out were performed to analyze the effects of diamond abrasive size on surface roughness. These experiments allowed the surface to be brought to sub-nanometer arithmetic average roughness *Sa*. The subsequent experiments were performed to analyze the effects of fine diamond, and colloidal silica on this sub-nanometer surface. The finishing conditions, that remained unchanged during the course of experimentation, are listed in Table 1.

TABLE 1 – EXPERIMENTAL CONDITIONS

Workpiece	Polycrystalline transparent YAG ceramic 
Linear motion travel distance	40 mm
Linear motion speed	1 mm/s
Drive magnet revolution	400 min ⁻¹
Clearance between table magnet and jig	1.16 mm

The center of the workpiece was found and designated as the origin of the Cartesian coordinates (Table 1). Surface roughness measurements were taken from the origin and every 1 mm for 10 mm in both the positive and negative x directions. These are the locations of the 21 measurements referred to in the following sections.

ROUGH POLISHING WITH DIAMOND ABRASIVE

The experiments presented in this section utilized 0.7 g of 44/149 μm diameter iron particles. Four different diamond abrasive sizes were used for this study. The 0-2 μm diameter diamond abrasive was used for 30 min and was followed by the 0-0.5, 0-0.25, and 0-0.1 μm diameter diamond abrasive for 60 min in series.

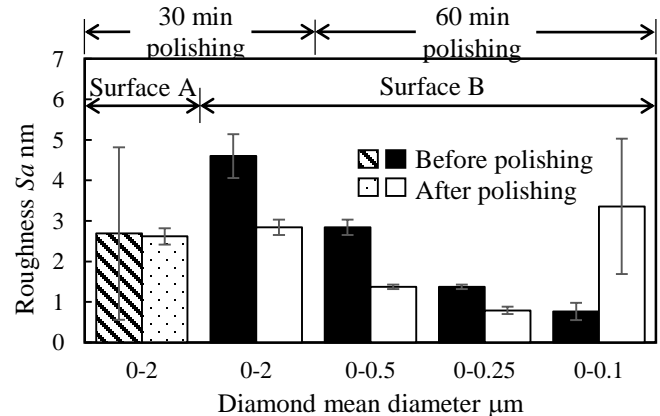
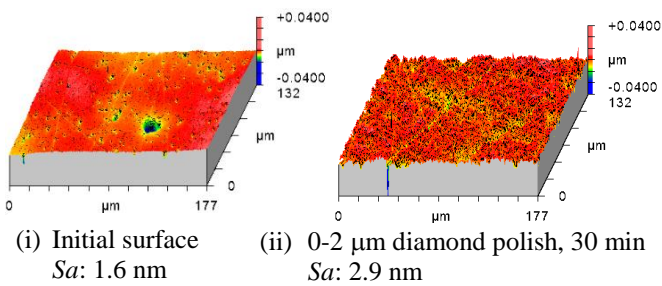


FIGURE 4 – RELATIONSHIP BETWEEN ABRASIVE SIZE AND ROUGHNESS

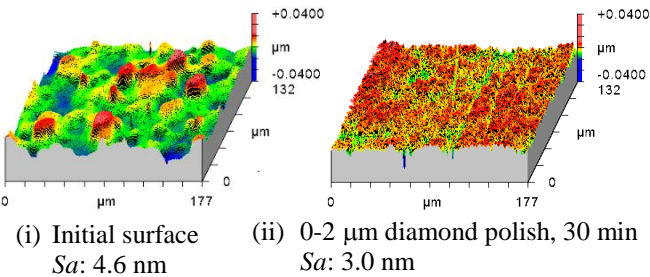
Figure 4 shows the roughness *Sa* averaged across all 21 measurement points, for the surface before and after every polishing stage. Polishing with 0-2 μm diameter diamond abrasive was performed for 30 min on two different surfaces with dissimilar initial surface conditions, referred to as Surface A and

Surface B. Figure 5 displays a three-dimensional oblique plot of a representative point from each surface. Surface A was heavily pitted and has a substantial standard deviation across the various measurements of the surface (Fig. 4). Surface B had many pillar like structures and an average roughness that is nearly double that of Surface A. After the process was performed both surfaces had very similar roughness values with a very low standard deviation across the measurement points. The remaining polishes presented in Fig. 4 were subsequently performed on the sample with Surface B.

As the diamond abrasive size was stepped down, the roughness decreased and the standard deviation stayed relatively small, showing the uniformity of the surface. After a 60 min polish with the 0-0.25 μm diameter diamond abrasive the surface roughness reached sub-nanometer levels. However, it was found that once the diamond abrasive size dropped to 0-0.1 μm , the roughness jumped up substantially and did not continue to decrease. The standard deviation of the measured data points also increased substantially suggesting that the effect was not uniform across the surface. To better understand the mechanisms behind this behavior, subsequent experiments were performed on the effects of polishing this material with very fine diamond abrasive once the surface had already achieved sub-nanometer levels.



(a) Surface A



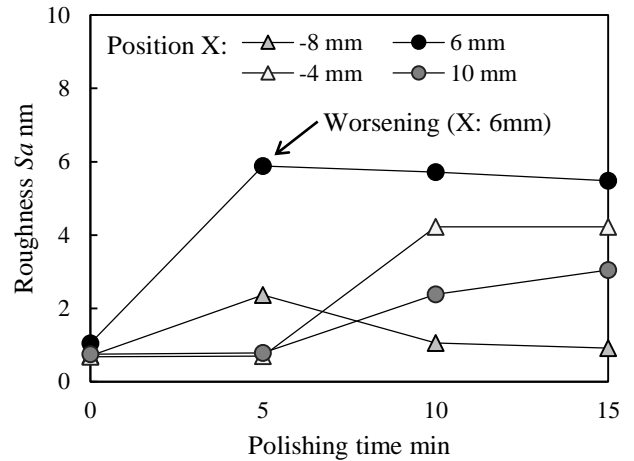
(b) Surface B

FIGURE 5 – THREE-DIMENSION OBLIQUE PLOTS OF SURFACE, ROUGH POLISHING

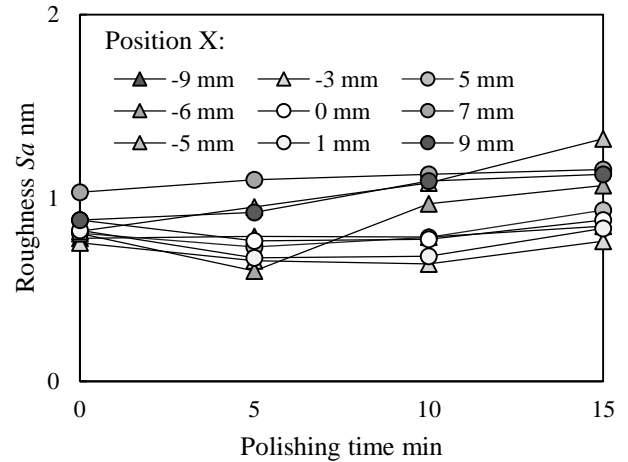
FINE POLISHING WITH DIAMOND ABRASIVE

The surface of the workpiece was returned to the sub-nanometer scale, using the 0-0.25 μm diameter diamond abrasive polishing process described in the previous section. The workpiece was then polished in 5 min increments using the 0-0.1 μm mean diameter diamond abrasive.

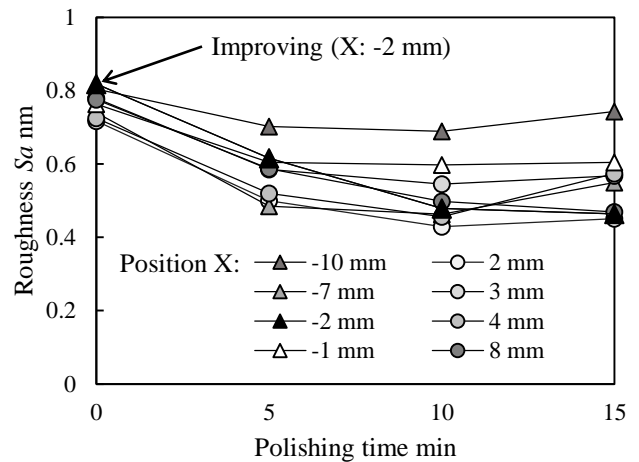
The roughness values at all 21 measured positions after each 5 minute polish are shown in Fig. 6. The positions on the surface that showed a dramatic worsening during the polishing series are



(a) Positions with dramatic worsening



(b) Positions with gradual average worsening



(a) Positions with gradual average improvement

FIGURE 6 – RELATIONSHIP BETWEEN POLISHING TIME AND ROUGHNESS, FINE DIAMOND ABRASIVE

displayed in part (a) of Figure 6. The positions that saw an average gradual worsening of the surface and the positions that saw an average gradual improvement are displayed in parts (b) and (c), respectively.

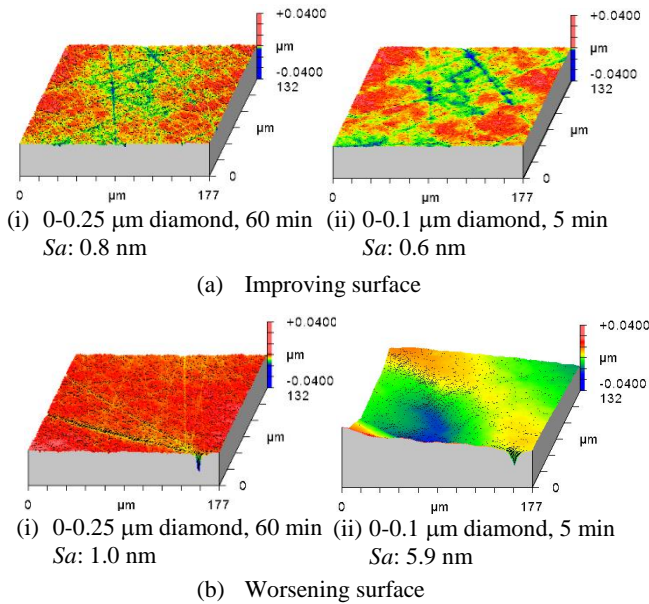


FIGURE 7 – THREE-DIMENSION OBLIQUE PLOTS OF SURFACE, FINE DIAMOND ABRASIVE

Figure 7 shows three-dimensional oblique plots of two locations on the surface, $X=-2$ mm (referred to as *Improving position*) and $X=6$ mm (referred to as *Worsening position*), respectively. The improving position is a representative surface of a measurement position that continued to improve with each subsequent polishing stage. After the 0-0.25 μm diameter diamond abrasive process, the surface at the improving position had a roughness of 0.8 nm S_a . The deepest valley was measured to be 12.5 nm, and the deeper scratches were relatively evenly distributed across the surface at this position. After polishing with the 0-0.1 μm diameter diamond abrasive for 5 min, the roughness improved to 0.6 nm and continued to improve after 10 and 15 min of polish time.

The worsening position, a representative surface of a measurement position that showed a dramatic worsening, had a higher initial roughness after polishing using the 0-0.25 μm diameter diamond abrasive (1.0 nm S_a). The deepest valley at this position was measured to be 27.7 nm, and two relatively deep scratches were located in close proximity. After polishing with the 0-0.1 μm diameter diamond abrasive for 5 min, a large section of material was removed from the area between these deep scratches. The abrasive was able to penetrate deeper into the valleys, and the iron particles continuously pushed and dragged these abrasive particles across the workpiece surface. Eventually, the localized force was able to cause a rupture. The roughness at this position worsened dramatically as a result, however it improved gradually with each additional 5 min process. After the chipping occurred the sharp edges of the chip

zone were smoothed, and this caused a leveling of the surface and thus a drop in the roughness value. In areas without substantial localized defects the step down in abrasive size continued the trend described in the previous section and improved the surface.

Due to the nature of mechanical polishing, internal stresses can build, and localized defects can continue to form causing a continuous process of chipping and smoothing. At this level of roughness, the chipping that occurred during the polish had a much more dramatic effect on the roughness values of the surface than the subsequent smoothing that this size abrasive could produce. As such, the surface roughness averaged across all measured points continued to climb with additional polish time. The standard deviation of the measured values also climbed with polishing time showing the unevenness of this effect across the surface.

FINE POLISHING WITH COLLOIDAL SILICA

To better understand the polishing effects of colloidal silica on transparent YAG ceramics a series of polishing tests were performed using a slurry of 3 wt% silica particles (7 nm mean diameter) in deionized water. The surface of the workpiece was again returned to sub-nanometer conditions by 0-0.25 μm diameter diamond abrasive polishing. In the first set of experiments three decreasing sizes of iron particles were used (44, 7, and 1 μm mean diameter) with 5 min process for each size.

Figure 8 displays the roughness, averaged across all 21 measurement points, for the surface after every polishing stage. The average roughness increases with each additional polish.

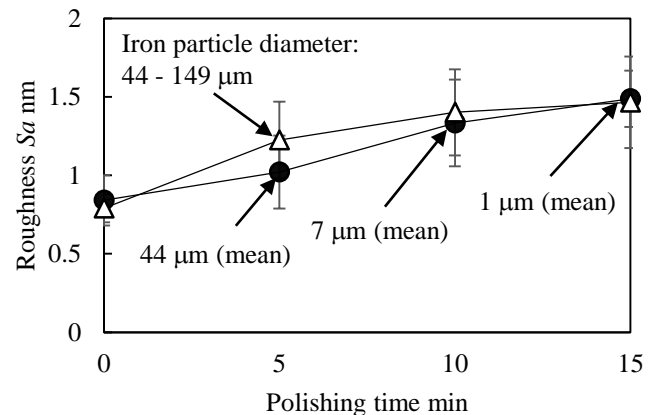


FIGURE 8 – RELATIONSHIP BETWEEN POLISHING TIME AND ROUGHNESS, COLLOIDAL SILICA

Figure 9 displays the topography of the center position of the surface after each polishing stage. As seen from Fig. 9 (a) and Fig. 9 (b), after the 5 min silica process with 44 μm mean diameter iron particles, while minor scratches began to dissipate, larger defects began widening during this process. The colloidal silica appeared to evenly remove material from the peaks and valleys of the surface. This resulted in little change in the depth

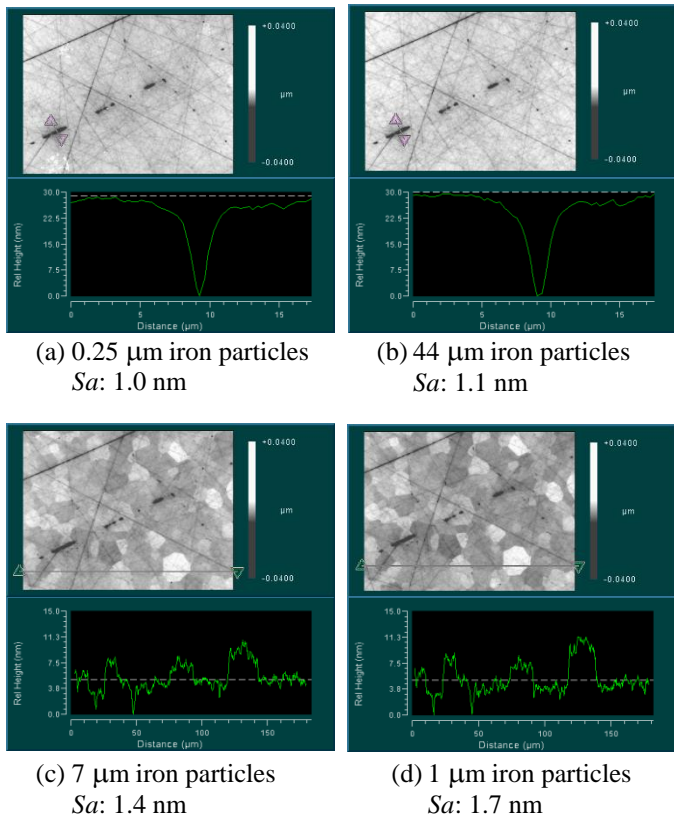


FIGURE 9 – TOPOGRAPHY OF ORIGIN, COLLOIDAL SILICA WITH VARYING IRON SIZE

of valleys. However, the width of the defects grew. This caused the general increase in the roughness value of the surface.

After a process was performed with the 7 μm mean diameter iron particles, the grains of the polycrystalline ceramic became apparent. This effect was further intensified as a result of the polish with the 1 μm mean diameter iron particles. The grain size of this polycrystalline ceramic was found to be between 15 and 30 μm . The grain structure of the ceramic influenced the material removal as the iron particle size dropped below the material's grain size.

The force pressing the colloidal silica against the surface of the workpiece drives the material removal. When the iron particle diameter is larger than the grain size, the force, generated by the single iron particle, pressing the colloidal silica against the workpiece surface is distributed across several grains. Thus, the material removal rate is even across multiple grains. However, when the iron particle diameter drops below the size of the grains, the iron particles can supply localized force within individual grains. This results in varying material removal rates between grains. Moreover, the small iron particles can supply force directed at individual grain boundaries. As material is removed from the naturally weaker boundaries, the small iron particles can penetrate into the resulting cavities resulting in increased material removal at these sites. This uneven material removal between grains, and increased removal at the grain boundaries, caused the grain structure of the YAG ceramic

workpiece to become increasingly apparent with additional polishing time. This increases the roughness of the surface.

Large iron particle sizes (44-149 μm) were then selected for further experiments to explore the effects of iron particle size on the material removal characteristics. The workpiece surface was once more returned to the sub-nanometer roughness conditions that were a result of 0-0.25 μm diameter diamond abrasive polishing. Measurements of the surface roughness were taken after subsequent 5 min process with this setup. The results are included in Figure 8. It was seen that roughness increased with time at a similar rate compared to the 44 μm iron particle experiment. Again, it became apparent that using 44-149 μm iron particles, larger than the ceramic grain size, with colloidal silica caused the widths of defects to grow and roughness to rise with polish time.

CONCLUSION

The results of this study can be summarized as follows:

1. A combination of a Nd-Fe-B tool magnet with a rubber magnet cap is required for the polishing of transparent YAG ceramics with MAF. A strong magnet was necessary for producing the magnetic force required to drive the tool magnet over the target surface. A rubber magnet cap with a diameter larger than that of the tool magnet was necessary to prevent iron particle motion, maintaining the iron particle brush between the tool magnet and workpiece surface.
2. MAF smooths transparent YAG ceramics with diamond abrasive to sub-nanometer levels despite large variability in initial surface conditions. However, polishing the ceramic with extremely fine diamond abrasive after the surface is already at sub-nanometer roughness values causes roughness to rise with polishing time as a result of a continuous cycle of chipping and smoothing. At this level, the chipping has a much more dramatic effect on the surface than the subsequent smoothing the fine abrasive can provide.
3. At sub-nanometer levels, MAF with colloidal silica abrasive caused a widening of defects with increased polish time, resulting in worsening roughness. When polishing is performed with iron particles smaller than the grain size of the YAG ceramic, uneven material removal between grains and increased removal at grain boundaries caused the grain structure of the YAG ceramic workpiece to become increasingly prevalent with additional polishing time.

ACKNOWLEDGMENTS

This material is based upon work supported by the Air Force Office of Scientific Research (AFOSR) under Award No. FA 9550-14-1-0270. The authors would also like to express their thanks to Dr. Akio Ikesue for showing his support by providing workpieces for experimentation.

REFERENCES

- [1] Maiman, T. H., 1960, "Stimulated Optical Radiation in Ruby," *Nature*, 187(4736), pp. 493-494.

- [2] Maiman, T. H., 1960, "Optical and Microwave-Optical Experiments in Ruby," *Phys. Rev. Lett.*, 4(11), pp. 546–566.
- [3] Geusic, J. E., Marcos, H. M., and Van Uitert, L. G., 1964, "Laser oscillations in Nd-doped yttrium aluminum, yttrium gallium and gadolinium garnets," *Appl. Phys. Lett.*, 4(10), pp. 182–184.
- [4] de With, G., and van Dijk, H. J. A., 1984, "Translucent Y₃Al₅O₁₂ ceramic," *Master. Res. Bull.*, 19, pp. 1669–1674.
- [5] de With, G., and Mulder, C. A. M., 1985, "Translucent Y₃Al₅O₁₂ ceramics: electron microscopy characterization," 16, pp. 81–86.
- [6] Sekita, M., Haneda, H., Yanagitani, T., and Shirasaki, S., 1990, "Induced emission cross section of Nd:Y₃Al₅O₁₂ ceramics," *J. Appl. Phys.*, 67(1990), pp. 453–458.
- [7] Ikesue, A., Furusato, I., and Kumata, K., 1995, "Fabrication and optical properties of high-performance polycrystalline Nd:YAG ceramics for solid-state lasers," *J. Am. Ceram. Soc.*, 78(4), pp. 1033–1040.
- [8] Lu, J., Prabhu, M., Xu, J., Ueda, K., Yagi, H., Yanagitani, T., and Kaminskii, A. a., 2000, "Highly efficient 2% Nd:yttrium aluminum garnet ceramic laser," *Appl. Phys. Lett.*, 77(23), p. 3707.
- [9] Ikesue, A., 2002, "Polycrystalline Nd:YAG ceramics lasers," *Opt. Mater. Amst.*, 19(1), pp. 183–187.
- [10] Taira, T., and Paper, I., 2007, "RE 3 + -Ion-Doped YAG Ceramic Lasers," 13(3), pp. 798–809.
- [11] Yagi, H., Yanagitani, T., Takaichi, K., Ueda, K., and Kaminskii, A. A., 2007, "Characterizations and laser performances of highly transparent Nd³⁺: Y₃Al₅O₁₂ laser ceramics," *Opt. Mater. (Amst.)*, 29(10), pp. 1258–1262.
- [12] Ikesue, A., and Aung, Y. L., 2006, "Synthesis and Performance of Advanced Ceramic Lasers," *J. Am. Ceram. Soc.*, 89(6), pp. 1936–1944.
- [13] Lee, S. H., Kochawattana, S., Messing, G. L., Dumm, J. Q., Quarles, G., and Castillo, V., 2006, "Solid-state reactive sintering of transparent polycrystalline Nd:YAG ceramics," *J. Am. Ceram. Soc.*, 89, pp. 1945–1950.
- [14] Ikesue, A., Yoshida, K., Yamamoto, T., and Yamaga, I., 1997, "Optical Scattering Centers in Polycrystalline Nd:YAG Laser," *J. Am. Ceram. Soc.*, 80(6), pp. 1517–1522.
- [15] Ikesue, A., Aung, Y. L., Taira, T., Kamimura, T., Yoshida, K., and Messing, G. L., 2006, "Progress in Ceramic Lasers," *Annu. Rev. Mater. Res.*, 36(1), pp. 397–429.
- [16] Fu, Y., Li, J., Liu, Y., Liu, L., Zhao, H., and Pan, Y., 2015, "Influence of surface roughness on laser-induced damage of Nd : YAG transparent ceramics," *Ceram. Int.*, 41, pp. 12535–12542.
- [17] Marinescu, I. D., Uhlmann, E., and Doi, T., 2007, "Mechanochemical Polishing and Chemical Mechanical Polishing," *Handbook of Lapping and Polishing*, CRC Press., pp. 292–301.
- [18] Golini, D., Jacobs, S., Kordonski, W., and Dumas, P., 1997, "Precision optics fabrication using magnetorheological finishing," *SPIE Proceeding: Advanced Materials for Optics and Precision Structures*, pp. 251–274.
- [19] Yamaguchi, H., Yumoto, K., Shinmura, T., and Okazaki, T., 2009, "Study of finishing of wafers by magnetic field-assisted finishing," *J. Adv. Mech. Des. Syst. Manuf.*, 3(1), pp. 35–46.